LU TP 00–01
January 11, 2000

A Model for the Colour Form Factor of the Proton

Master of Science Thesis by Johann Dischler
Thesis advisor: Torbjörn Sjöstrand
Department of Theoretical Physics,
Lund University, Lund, Sweden

Abstract

The total cross-section σ_{tot} and the jet cross-section σ_{jet} differ at a proton-proton collision. The latter is divergent if arbitrarily small transverse momenta are allowed. Even with some fixed lower $p_\perp$ cutoff, σ_{jet} increases much faster than σ_{tot} at high energies. We have in this paper studied how the divergence could be tamed by colour screening effects among the partons.
To do this we have built a proton model where we assign momenta, positions and colour charge to all partons in the proton.
We find that the relative behaviour of the cross-sections can be better understood by the inclusion of this effect.

1 Introduction

The Standard Model is the theory that all modern particle physics is based on. It tells you which particles that exist and how these particles interact with each other. The Model divides the particles into two main groups, matter particles and gauge bosons. As the name indicates, all matter is built up from the matter particles. The gauge bosons are the particles that mediate the interactions "forces" between the matter particles and themselves. The matter particles are divided in two different groups, the quarks and the leptons. These, in their turn, are placed in groups called families according to:

$$\begin{pmatrix} \mathrm{u} \\ \mathrm{d} \end{pmatrix} \quad \begin{pmatrix} \mathrm{c} \\ \mathrm{s} \end{pmatrix} \quad \begin{pmatrix} \mathrm{t} \\ \mathrm{b} \end{pmatrix} \tag{1}$$

$$\begin{pmatrix} \nu_\mathrm{e} \\ \mathrm{e} \end{pmatrix} \quad \begin{pmatrix} \nu_\mu \\ \mu \end{pmatrix} \quad \begin{pmatrix} \nu_\tau \\ \tau \end{pmatrix} \tag{2}$$

The upper ones are the quarks and they are named up, down, charm, strange, top and bottom. The quarks u, c, t all have $(2/3)e$ in electric charge and d, s, b have $-(1/3)e$. All the matter that we have around us is made up of only the first family, that is up and down; the rest of the quarks exists today only inside accelerators and in some very energetic cosmic objects.

The particles in Eq (2) are the leptons. The most famous of the leptons is the electron, but there are five more. The electron e, the muon μ and the tau τ all have electric charge $-e$, while the neutrinos ν are electrically neutral.

Then there are the gauge bosons that mediate the different forces between the particles. There are four fundamental forces in the universe:

Interaction	Gauge bosons
gravitation	graviton
electromagnetic	γ
weak	$\mathrm{W}^+, \ \mathrm{W}^-, \ \mathrm{Z}^0$
strong	$\mathrm{g}_i, \ \ i = 1 \ldots 8.$

(3)

Gravitation interacts with all matter, but it is so weak that it can be neglected almost always in particle physics. Then there is the electromagnetic force which is responsible for holding the atom together. The weak force is e.g. responsible for the β-decay in the nuclei. In the standard model one has succeeded to combine the electromagnetic and the weak forces to one—the electro-weak force. And last there is the strong force that holds the quarks and nucleons together [1].

In this paper we are going to look at the strong force and its gauge-bosons, the gluons, so a deeper study of this is in order. The strong charge is called colour-charge. Instead of $+$ and $-$ there is red, blue, green and their anti-colours antired, antiblue and antigreen. All matter in the universe is built up of the quarks and the leptons. The quarks can't exist in isolation, but must be combined in colour-singlet states. This can be done in two main ways. You can combine a quark (colour) with an anti-quark (its anti-colour), this is called a meson, or you can take one quark of each colour (e.g. red-green-blue), this is called a baryon. The gauge bosons of the strong force, the gluons, can themselves carry colour charge. This means that the emission or absorption of a gluon can change the colour of the quarks as seen in Fig. 1. The gluons have colour charge either as colour and

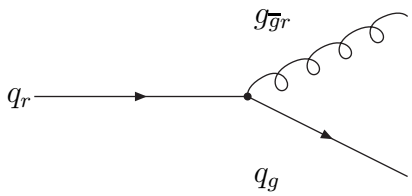

Figure 1: A gluon can change the colour of a quark

a different anticolour (e.g.red-antiblue,$r\overline{b}$) or are in colour neutral states (e.g.$\frac{1}{\sqrt{2}}(r\overline{r}-g\overline{g})$).

Almost all research in particle physics is done at huge accelerators. One is located near Chicago, called the Tevatron, and it is part of a research center called Fermilab. The accelerator ring is buried under the ground in a tunnel that has a circumference of about 6 km. Here one collides protons (or actually protons and antiprotons) at energies as high as $E_{CM} = 1.8$ TeV.

It is such collisions that we are going to study in this paper, or a bit more exactly, the cross-section of proton-proton collisions [2]. The cross-section is a measure of how probable a reaction is. One can think of it as an effective radius of the incoming particles. If the two incoming particle's "radii" overlap each other we have an interaction. In our case we confront two different cross-sections, the proton-proton total cross-section σ_{tot} and the one called σ_{jet}. In σ_{jet} we look at the particles inside the proton and their collisions instead. The particles inside the proton are usually called partons, and these include both quarks and gluons. It is these collisions between the partons that one can calculate theoretically. From these calculations one can create a theoretical σ_{tot} that you can compare with the experimental total cross-section. The measured cross-section increases much slower with the energy than the theoretical. There already exists some explanations to this, such as multiple interactions, see Section 2.2, but these are not enough to explain the gap between the experimental data and the theoretical predictions.

What we have done is to build a simple model of a proton with all its particles, partons. We have for all these partons calculated the momenta, positions and the colour-charges. We have also constructed the model so that the whole proton must be colour-neutral. What we are hoping to see is that the partons will screen each other and thereby the cross-section will be reduced. If the energy is high, the number of partons is large and this screening effect should be bigger. That is, the increase of the cross-section should be slower, which is exactly what is desired. We show that such a screening indeed appears to be an important physical mechanism.

This paper is organized as follows: We will in Chapter 2 make some theoretical arguments about the evolution of our proton model and discuss the screening effect. In Chapter 3 we will describe our model for the proton. Later in Chapter 4 we uses this model to observe how a gluon interacts with a proton. And last in Chapter 5 we summarize and give some conclusions.

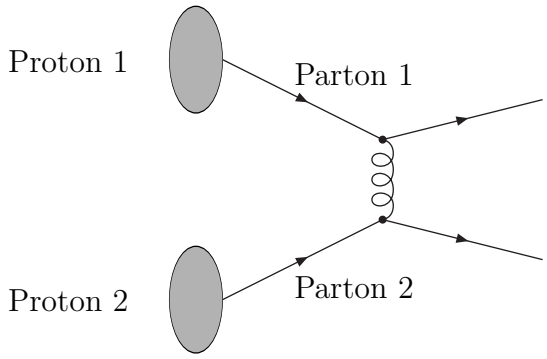

Figure 2: A proton-proton interaction where two partons scatter against each other

2 Theory

If we collide two protons with each other, see Fig. 2 , we have a parton-parton cross-section according to:

$$\mathrm{d}\sigma_{jet} = \int \mathrm{d}x_1 f(x_1, Q^2) \int \mathrm{d}x_2 f(x_2, Q^2) \int \frac{\mathrm{d}\hat{\sigma}}{\mathrm{d}p_\perp^2} \mathrm{d}p_\perp^2. \tag{4}$$

The first integral factor in Eq (4) expresses the flux of partons from proton 1. The second term is then the flux of partons from proton 2. The last term is a measure of the actual probability that two partons will interact with each other.

The parton function $f(x, Q^2)$ expresses the probability to find a parton with momentum fraction x of the incident proton momentum, while Q sets the virtuality scale at which the proton is probed. Q is often in hadron-hadron collisions represented by $p_\perp$ since these variables scale approximately the same, that is

$$\mathrm{d}\sigma_{jet} = \int \mathrm{d}x_1 f(x_1, p_\perp^2) \int \mathrm{d}x_2 f(x_2, p_\perp^2) \int \frac{\mathrm{d}\hat{\sigma}}{\mathrm{d}p_\perp^2} \mathrm{d}p_\perp^2. \tag{5}$$

The parton functions $f(x_i, p_\perp^2)$ in Eq (5) increase very fast at small x-values (see Section 2.1 for further details), that is small momentum for the partons. They also increase for bigger virtuality, Q. This will eventually lead to a parton-parton cross-section that is bigger than the whole proton-proton cross-section.

2.1 Evolution Equations

When you are studying how a hadron, e.g a proton, is built up you have to do this by sending a particle, a probe, at the hadron. This probe then scatters against a parton inside the hadron and by this you can draw conclusions about how the hadron is made up. If the probe has a large Q (is very virtual) it can resolve more details and we see more partons.

That there are details to resolve is a consequence of the quantum mechanical fluctuations. Virtual fluctuations $a \to bc \to a$ appear and disappear continuously, with lifetimes related to the virtuality scale according to the Heisenberg uncertainty principles. The fluctuations can be nested, thereby giving rise to whole cascades of fluctuations.

There are three different processes that can happen in the parton cascade. These are the three vertices of the strong interaction of the first order. A quark can split into a quark and a gluon. And a gluon can either split into a quark-antiquark pair or into two gluons, see Fig. 3. These processes are of course reversible, so e.g a quark can absorb a gluon.

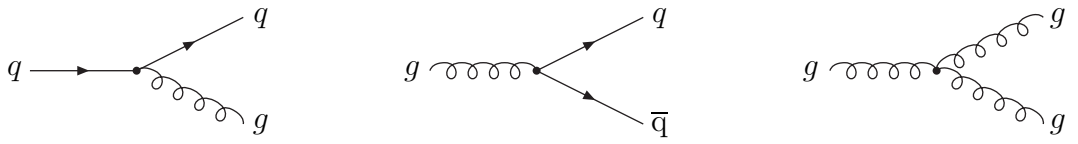

Figure 3: The 3 main vertices in the strong interaction

The daughters share the momentum of the mother between themselves according to some probability distributions. It is e.g. a large probability that the gluon emitted by the quark has very small momentum. These probability distributions are described by the Altarelli-Parisi splitting kernels [3]

$$P_{\mathrm{q}\to\mathrm{qg}}(z) = \frac{4}{3}\frac{1+z^2}{1-z}, \tag{6}$$

$$P_{\mathrm{g}\to\mathrm{gg}}(z) = 3\,\frac{(1-z(1-z))^2}{z(1-z)}, \tag{7}$$

$$P_{\mathrm{g}\to\mathrm{q\overline{q}}}(z) = n_{\mathrm{f}}\,\frac{1}{2}\,(z^2+(1-z)^2), \tag{8}$$

where n_{f} is the number of allowed flavors, usually 3-5. The variable z is the fraction of the mother momentum that the first daughter takes (i.e. the quark in Eq (6)). The other daughter then gets $(1-z)$ of the momentum. Both in Eq (6) and Eq (7) there are singularities, in Eq (6) at $z=1$ and in Eq (7) both at $z=1$ and $z=0$. The physical explanation is that there, at any given time, is a cloud of gluons with very low momenta around a quark. In reality even if there are are infinitely many gluons so are their total momentum finite. One usually introduce a cutoff, z_{min}, and branchings that includes gluons below this z_{min} (or over $(1-z_{min})$) are then not allowed.

The probability that we will have a branching a $\rightarrow$ bc at all is given by the evolution equation, the DGLAP equation [3]:

$$\frac{\mathrm{d}P_{\mathrm{a}\rightarrow\mathrm{bc}}}{\mathrm{d}(\ln Q^2)} = \int \mathrm{d}z \frac{\alpha_s(Q^2)}{2\pi} P_{\mathrm{a}\rightarrow\mathrm{bc}}(z) \tag{9}$$

or, if one introduces the evolution parameter $t = \ln \frac{Q^2}{\Lambda^2}$

$$\frac{\mathrm{d}P_{\mathrm{a}\rightarrow\mathrm{bc}}}{\mathrm{d}t} = \int \mathrm{d}z \frac{\alpha_s(t)}{2\pi} P_{\mathrm{a}\rightarrow\mathrm{bc}}(z). \tag{10}$$

That is, for a small increase in t, $\mathrm{d}t$, there is a probability $\mathrm{d}P$ that a branching a $\rightarrow$ bc will take place. So the evolution equation evolves in the virtuality, Q. This does not mean that the individual partons evolve in Q, but it is simply an easy way to pick the right value for the branchings at which the partons are resolved.

Another way of expressing this is an inclusive picture; you could calculate the probability of finding a parton at a certain x value. This becomes more like a mean-value of the distribution, but it is a picture that is often used since it is these distributions that you can measure at experiments, and not how a single parton develops. We have, for the inclusive picture, the following expression:

$$\frac{\mathrm{d}f_i(x)}{\mathrm{d}(\ln Q^2)} = \int_x^1 \mathrm{d}y f_j(y) \int_0^1 \mathrm{d}z \frac{\alpha_s}{2\pi} P_{\mathrm{j}\rightarrow\mathrm{ik}}(z)\, \delta(yz - x). \tag{11}$$

The first integral in Eq (11) simply says that the mother, j, has to have at least x momentum. The other integral one recognizes from our earlier expression in Eq (9), and the delta function ensures that the daughter, i, obtains x in momentum. If we use the delta function to eliminate one of the integrals we get

$$\frac{\mathrm{d}f_i(x)}{\mathrm{d}(\ln Q^2)} = \int_x^1 \frac{\mathrm{d}y}{y} f_j(y) \frac{\alpha_s}{2\pi} P_{\mathrm{j}\rightarrow\mathrm{ik}}\left(\frac{x}{y}\right). \tag{12}$$

So this expresses number of daughters that will get x momentum from a mother of momentum higher than x. But these partons with x momentum can also decay, so we have also an out going flow from this point that has to be subtracted from the expression.

Once you have a parton distribution at some Q-scale you can by these evolution equations iterate towards higher Q and get the whole distribution above this Q. This has been done by many groups [4, 5] for different starting values. One feature that is common for all groups is that the distributions are very high at small x-values.

2.2 Multiple Interaction

If two protons collide with each other it can happen that more than one pair of partons collides inside the protons. This we call multiple interaction [6]. There are some experimental data that indicates this phenomena [7, 8].

The total cross-section, σ_{tot}, is of the order $40 - 70$ mb see Fig. 4. It is often parameterized according to [9]:

$$\sigma_{tot} = As^{-\eta} + Bs^{\epsilon}, \tag{13}$$

where s is the E_{CM} squared, $\eta \sim 0.5$ and $\epsilon \sim 0.08$.

Let us, on the other hand, look at the parton-parton cross-section, and make some rough estimates such as: $f_i(x,t) \sim x^{(-1-\epsilon')}$, and introduce an x_{min} to avoid to get singularities at $x = 0$ and finally a $p_{\perp min}$. $p_{\perp min}$ is introduced as an integration limit that you after calculating the integral should put to zero. If you do all this you will get something like:

$$\begin{aligned} \sigma_{jet} &= \int \mathrm{d}x_1 f(x_1, Q^2) \int \mathrm{d}x_2 f(x_2, Q^2) \int \frac{\mathrm{d}\hat{\sigma}}{\mathrm{d}p_\perp^2} \mathrm{d}p_\perp^2 \\ &\sim \left(\frac{1}{x_{min}^{\epsilon'}}\right)^2 \frac{1}{p_{\perp min}^2} \sim \frac{s^{\epsilon'}}{p_{\perp min}^2}. \end{aligned} \tag{14}$$

As is clearly seen, one must have $p_{\perp min} \neq 0$. This contradiction can, we hope, be explained by the screening effect, see the next section. If you do these calculations a bit more carefully, or uses a simulation program such as PYTHIA 6.1 [10] you get curve according to Fig. 4. One can increase $p_{\perp min}$ but this will only move the problem to another region.

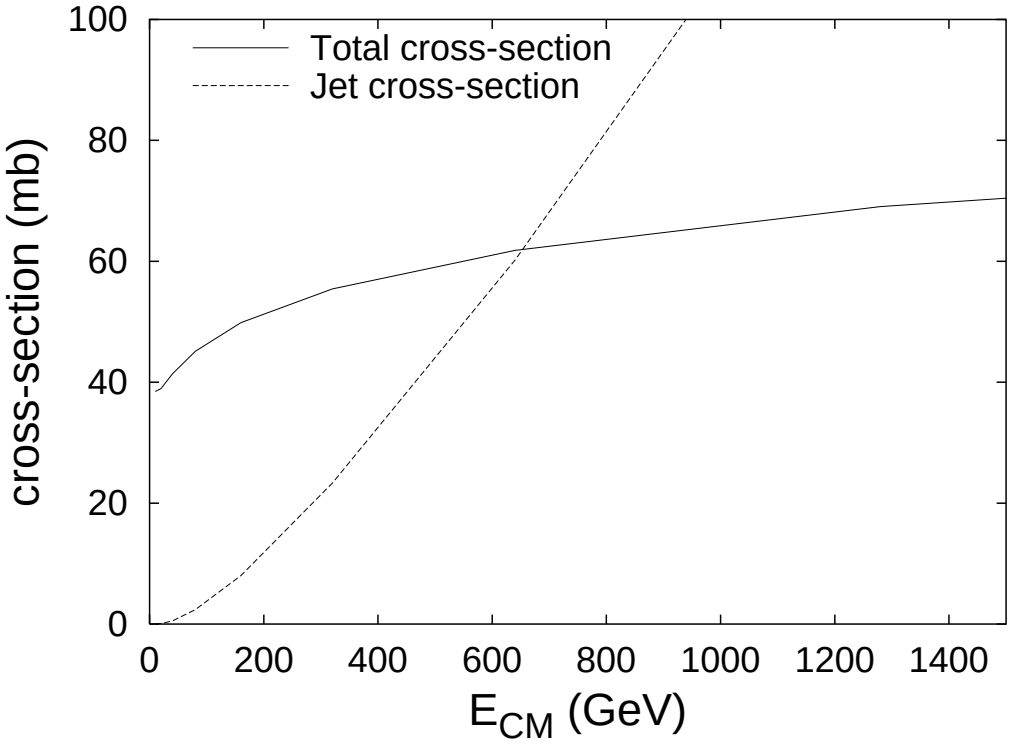

Figure 4: The total cross-section σ_{tot} and the parton-parton cross section σ_{jet}. $p_{\perp min}$ is here set equal to 2 GeV

The huge difference between the two curves can, in part, be explained by multiple interaction since we have:

$$\sigma_{tot} = \sigma_{0jetpair} + \sigma_{1jetpair} + \sigma_{2jetpairs} + \cdots, \tag{15}$$

$$\sigma_{jet} = \sigma_{1jetpair} + 2\sigma_{2jetpairs} + 3\sigma_{3jetpairs} + \cdots, \tag{16}$$

where we have to multiply by the number of jets in σ_{jet} because $\sigma_{ijetpair}$ tells about the probability to have i jet pairs. If we have i jet pairs we always has i such terms.This leads to that at an event with many jets (high energy) the σ_{jet} will be higher than σ_{tot}.

This seems to explain the curves well, but unfortunately it's not enough. We believe that the necessary last correction can be explained by the screening effect, that is that the quarks will not interact as if they are free particles which has been assumed in the perturbation calculations of the σ_{jet} cross-section.

2.3 Screening effect

All hadrons are in colour singlet states. This means that if you can't resolve a hadron it will not interact strongly. That is if you e.g. send a gluon with a very long wavelength at a proton, the gluon will not be able to see the partons inside the proton, but only the proton as a single object. Since this object is in a colour singlet state the gluon will have problem to interact with it. On the other hand, if the gluon is very energetic and has a short wavelength, it will resolve much more partons and the screening effect will become much smaller.

This can be studied by looking at the ratio A between the incoherent and the coherent sum of colour charges in the cascade.

$$A = \frac{|\sum_{k=1}^{n} q_k e^{ipx_k}|^2}{\sum_{k=1}^{n} |q_k|^2}. \tag{17}$$

Here is n the number of partons in the proton, q_k is the colour charge of the k:th parton and x_k is the position of the k:th parton. The gluon has a momentum of p. If the gluon has a low p the wavelength is so long that it won't matter where in the proton the partons are, see Fig 5, and all terms will cancel. Or you could see it like this: if $p \to 0$ then $A \to 0$ (since $\sum q_k = 0$) and if $p \to \infty$ then $A \to 1$

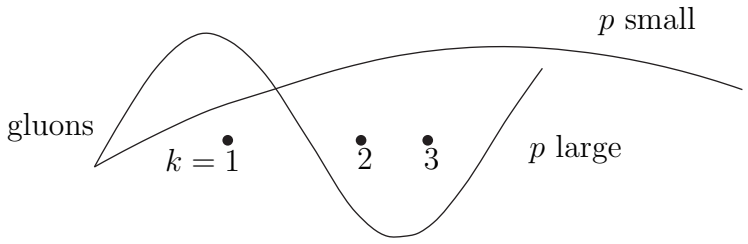

Figure 5: The screening effect; A gluon interacts with the partons in a proton and depending on the wavelength it interacts differently.

3 The Proton-Model

We start, in our model of the proton, at a very low virtuality scale Q. At this low Q we assume that we have a finite number of partons, or more specificly, that we have 3 quarks and 2 gluons [11]. These 5 partons are then evolved to higher Q by Eq (10) to some Q_{max}. As we do this we continuously assign each new parton with momentum, position and colour charge according to some given probability. We have decided the transversal position of the partons while in the momentum space the longitudinal momentum is selected. We do this since it allows us to build a model and still be consistent with the Heisenberg Uncertainty Principle. To have a colour-neutral proton we, to begin with, have a colour-neutral start configuration, but then as we evolve we keep all partons. To avoid getting too many partons we had to introduce a x_{min} and branchings in which a parton had a momentum under this were not allowed. This rather abrupt cutoff did not change the distribution significantly, as we shall see.

3.1 Start configuration in momentum space

We choose to start with 3 quarks and 2 gluons. In this choice we were guided by other works done earlier. In the original in 1976 [12] one started with only the three valence quarks, and this was not enough to fit the data with experiments. The GRV group [11, 13] later made the assumption that you had to introduce some gluons and seaquarks already from the beginning, though only very few, and this seems to be sensible since they got a good fit to the experiments . We cannot use the GRV distribution itself, since they use a inclusive picture, while we need an exclusive picture to be able to assign momenta, colour charge etc. to all partons.

In our model, each parton was given a fraction x of the total momentum from a distribution that was fitted to give values similar to what the GRV group had. What we are trying to get is a qualitative picture of the parton distribution, not to compete with GRV for the best configuration. We made the following ansatz:

$$f(x) = Nx^{\alpha}(1-x)^{\beta}, \tag{18}$$

where N is a normalization factor to get the right number of partons and α and β are the free parameters that we used to adjust the distribution.

To get the proper normalization $\sum_{i=1}^{5} x_i = 1$ we made the following operation:

$$(x_i)_{\text{norm}} = \frac{x_i}{\sum_{j=1}^{5} x_j}. \tag{19}$$

This means that the original distribution is pushed towards the middle. As it were we had to choose $\alpha < 0$. Some trial and error finally gave that:

$$\begin{aligned} \alpha &= -0.4 \\ \beta &= 1.2 \end{aligned}$$

Though even this did not give a very good distribution. We had too much partons at high momentum and too few at low, see Fig. 6. This we solved by starting our evolution at $Q = 0.44$ instead of $Q = 0.48$ as they had done. That means that when we were at $Q = 0.48$ some of the partons with high momentum had split to two other partons with lower momentum and we got a good fit, see Fig. 6.

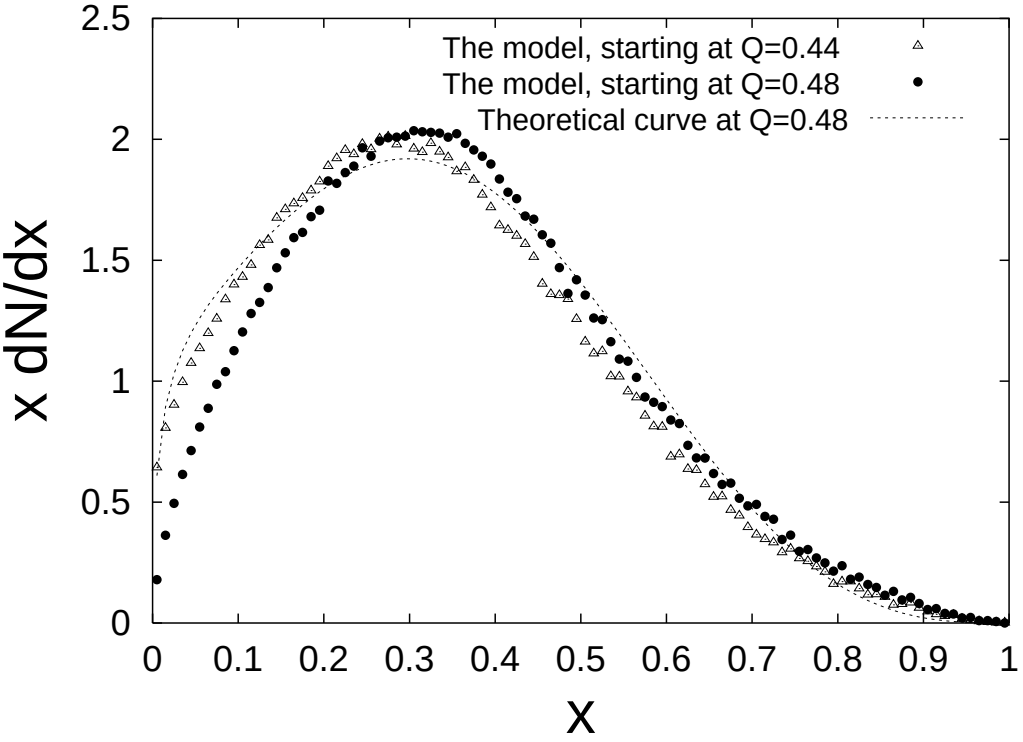

Figure 6: Different start configurations for the momentum. Theoretical curve from [11]

3.2 Start configuration in coordinate space

Our model is 2-dimensional. This is not a strong limitation, though, since the protons have a very high speed and thereby are strongly Lorentz-contracted. That is, they can with good approximation be taken to be 2-dimensional objects. And since the only thing that we are going to do is to send plane waves in the transverse direction of the beam at the proton, see Fig. 7, we can project the points onto the x-axis. So we put $x = r\cos\theta$ and chose θ at random for each new branching.

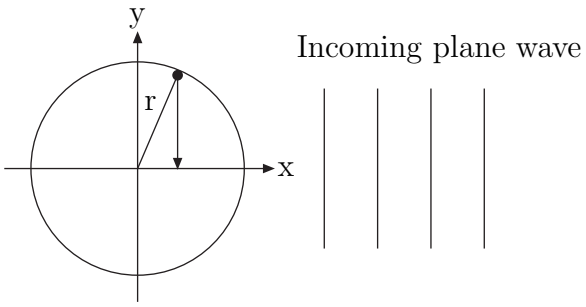

Figure 7: The projection of the position

We have introduced a characteristic radius, r_0, of the proton at $r_0 = 0.7$ fm. The 5 original partons are then randomly chosen according to some distribution. We tried some different distributions:

- Gauss : $f(r)\mathrm{d}r \propto \frac{1}{\sqrt{2\pi}r_0} e^{\frac{-r^2}{2r_0^2}} r\mathrm{d}r$

- Exponential I: $f(r)\mathrm{d}r \propto e^{-\frac{r}{r_0}} r\mathrm{d}r$
- Exponential II : $f(r)\mathrm{d}r \propto \frac{e^{-\frac{r}{r_0}}}{r} r\mathrm{d}r$

Here is r_0 the characteristic radius. The difference in the final results of the parton shower did not depend much on which of these distributions we choose. We decided to take the Gaussian distribution.

3.3 The evolution of the momentum

We have chosen to work with an exclusive picture, that is we follow the development of each parton in the proton. This picture is easy to work with since you can iterate from a start configuration of partons. You know the probability for a parton to split up at a little step, $\mathrm{d}t$, of the evolution parameter. So by using random numbers to simulate the probability of the splitting you can reproduce the actual process. In the exclusive picture we had:

$$\frac{\mathrm{d}P_{\mathrm{a}\to\mathrm{bc}}}{\mathrm{d}t} = \int_{z_{min}}^{1-z_{min}} \mathrm{d}z \frac{\alpha_s(t)}{2\pi} P_{\mathrm{a}\to\mathrm{bc}}(z), \tag{20}$$

with

$$\alpha_s = \frac{12\pi}{(33-2n_f)\ln(Q^2/\Lambda^2)} = \frac{12\pi}{25t}, \tag{21}$$

where $n_f = 4$ and $t = ln(Q^2/\Lambda^2)$. Since we have that $z_{min} = x_{min}/x$ we can't have any partons under x_{min}. For the quark channel $q \to qg$ this gives, with help of the Altarelli-Parisi splitting kernels to decide $P_{\mathrm{q}\to\mathrm{qg}}$, that the evolution equation looks as:

$$\frac{\mathrm{d}P_{\mathrm{q}\to\mathrm{qg}}}{\mathrm{d}t} = \frac{6}{25t} \int_{z_{min}}^{1-z_{min}} \mathrm{d}z \frac{4}{3} \frac{1+z^2}{1-z} \equiv \frac{C}{t}. \tag{22}$$

You can, by simply putting in the different splitting kernels, get the evolution equations for $g \to q\overline{q}$ and $g \to gg$. For a gluon you have to decide which of the channels it will take: either the gg or the $q\overline{q}$. This is randomly chosen according to the different probabilities of the channels.

The number of partons, N, at a given Q is then given by

$$\frac{\mathrm{d}N}{\mathrm{d}t} = -\frac{C}{t} N(t) \tag{23}$$

One can draw a parallel here to the exponential decay of a radioactive nucleon. It has a certain probability, P, to decay, but if you look at a large number of nucleons the probability that you will have a decay in a little time interval decreases as the time elapses since you have fewer nucleons left which can decay. By solving Eq (23) you get how many partons, N, you have at a given Q-scale.

In this way you evolve your parton distribution until you reach $Q = Q_{max}$. We have also introduced a x_{min} to keep the number of partons in our model from exploding. All branchings in which any of the daughters has a momentum less than x_{min} are forbidden.

We have compared our model with values from the GRV group [11], see Fig. 8 and Fig. 9. We have an excellent agreement if we include all partons, as seen in the upper curves . The antiquarks though are somewhat suppressed in our model, especially at low Q. This is not so strange, since we in our model assume that we don't have any

antiquarks in our start configuration and GRV have a mixture of them. At higher Q these differences shrink and the two curves approaches each other, see Fig. 9 . We have a fairly good agreement at low x-values also, see Fig. 10, and this is a bit surprising since we have introduced a x_{min} cut.

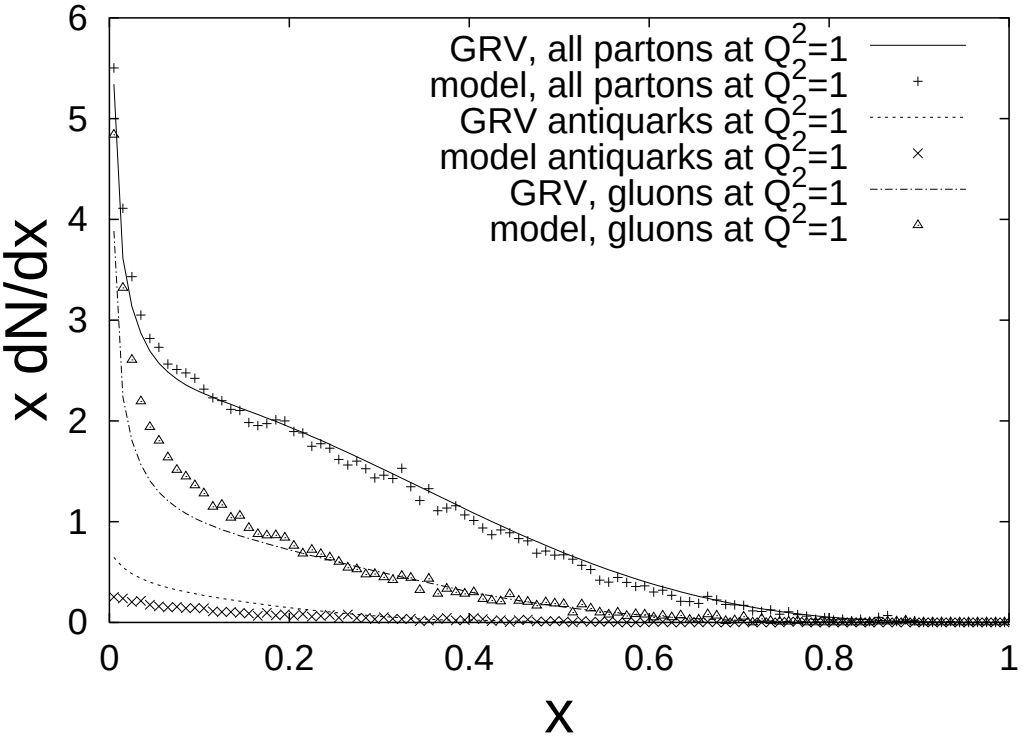

Figure 8: The evolution of the momentum at $Q^2 = 1$. At $Q^2 = 1$ $\overline{\mathrm{q}}$ is too low in our model. The quark distribution can be attained by subtracting the gluon and the antiquark distributions from the total.

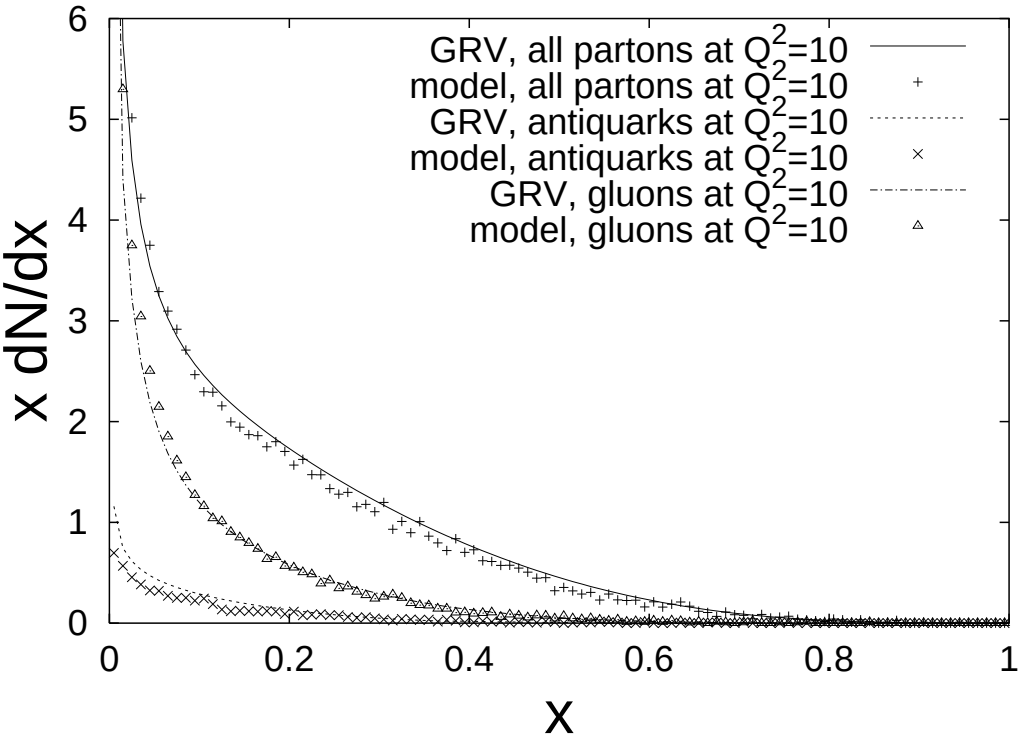

Figure 9: The evolution of the momentum at $Q^2 = 10$. The $\overline{\mathrm{q}}$ curve of our model has approached the theoretical curve.

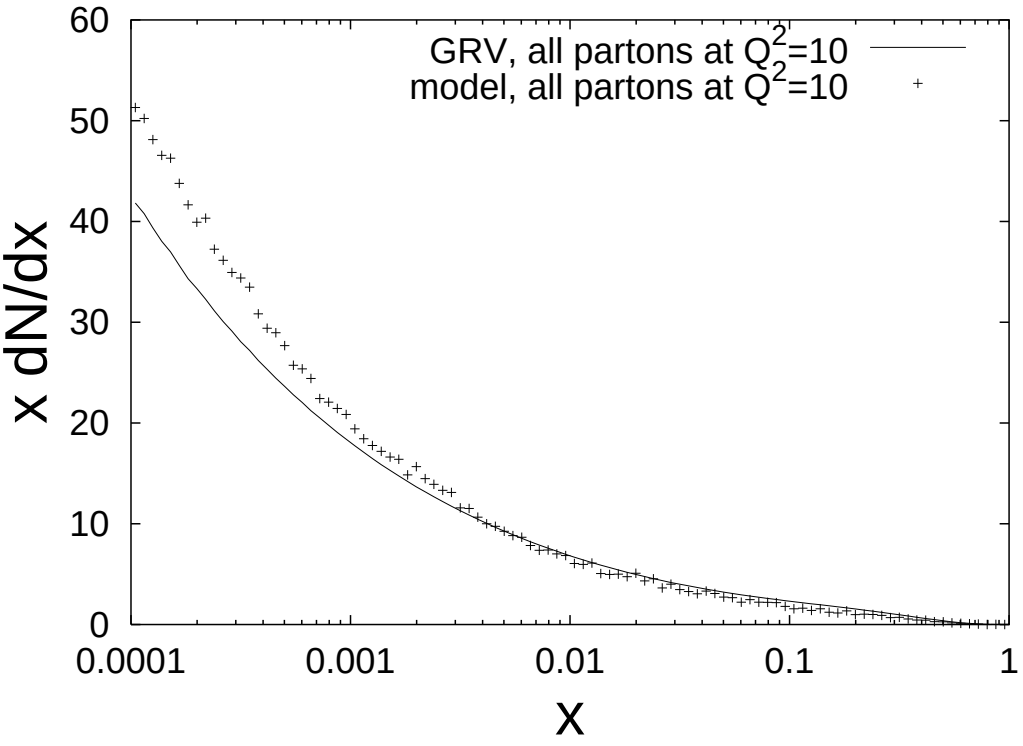

Figure 10: The evolution of the momentum at $Q^2 = 10$ in log scale. $x_{min} = 10^{-4}$

3.4 The evolution of the position

The distance a parton will reach from its origin of creation depends on a number of things. In our model we assign each new pair of partons with a distance, x, according to:

$$x = x_0 \pm \frac{\mathrm{R}}{Q} \cos\theta \sqrt{1 - z_i} \tag{24}$$

Here is x_0 the position of the vertex where the two partons were created and R is a random number between 0 and 1.

The first factor $\frac{1}{Q}$ comes from the Heisenberg Uncertainty Principle. A parton with high virtuality, Q, lives shorter than a parton that is almost real. The random number, R, is there since a parton has freedom to decay at any point between x_0 and forward to our maximum distance $\frac{1}{Q}$. We have experimented with this factor and chosen some different distributions. One, perhaps more physical, is that instead of choosing a random number linearly to chose them from a exponential distribution. This agrees with a quantum mechanical picture, it is a high probability that it decays early but there exists a chance that it will live very long.

The second factor in Eq (24) $\cos\theta$ is simply the projection of the partons position to the x-axis as discussed in section 3.2. The angle θ is randomly chosen.

The third and last factor comes from the kinematics of the system, according to Fig. 11. We have, from the conservation of energy and momentum, the following expressions:

$$(E + p_z)_1 = z(E + p_z)_0 \tag{25}$$

$$(E + p_z)(E - p_z) = m^2 + p_\perp^2 \tag{26}$$

Here p_z is the direction of the incoming particle and $p_\perp$ is the direction orthogonal to this. If we apply Eq (26) on the initial state (0) and the final state (1 and 2), we get

$$0 = \frac{-Q^2 + p_\perp^2}{(E + p_z)_1} + \frac{p_\perp^2}{(E + p_z)_2} = \frac{-Q^2 + p_\perp^2}{z(E + p_z)_0} + \frac{p_\perp^2}{(1 - z)(E + p_z)_0}. \tag{27}$$

In the last equality Eq (25) was used. From this expression it is straight forward to get a relation between $p_\perp$ and z according to:

$$p_\perp = \sqrt{1 - z}\; Q. \tag{28}$$

If a parton gets a large share, z, of the momentum it will not be able to deviate much from the original partons direction. Therefore the distance it will travel according to Eq (24) is small. We have also studied results without this factor, and find that it is not critical for the qualitative results.

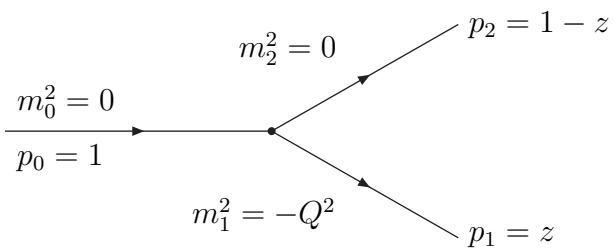

Figure 11: The kinematics of a vertex

3.5 The colour charge

Since the colour charge has 3 different charges (colours), instead of as in electromagnetism 2, you have to introduce one more dimension to represent the colour space. That is, you will get a colour-plane, Fig 12, where the different charges of the particles are added to each other as vectors. Though this is not completely true, since we have the same phenomena here as in the spin-space. Even though the z component, S_z, of the spin is zero the total spin, S, can be a finite value, since S_z is the projection of the spin vector on the z-axis. The same thing happens in the colour space, we can have a colour neutral particle that is not a colour singlet. An example of this are the two colour neutral gluons (e.g. $\frac{1}{\sqrt{2}}(r\overline{r} - g\overline{g})$). We don't make this distinction in our model though, and we treat the colour charge as if it simply were vectors in a two dimensional space. So, e.g. you get the gluon $g\overline{b}$ charge by adding the vectors of the green charge and the antiblue charge, and so on.

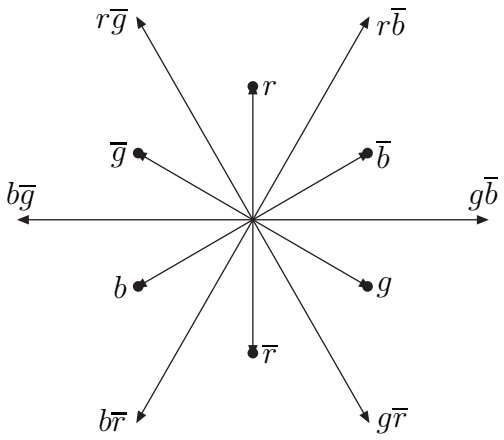

Figure 12: The representation of colour charge in a 2-dimensional room

This representation of the colour charge is not perfect, we have only 6 gluons, as is seen in Fig. 12. The colour neutral gluons (2) are not represented in this picture, since they would then coincide with origo which would give a set of none-interacting gluons. Another thing that is not entirely correct is the length, or charge, that the gluons get. In this representation the length of the gluons is $\sqrt{3}$ while it should be $\sqrt{\frac{N_c}{C_F}} = \sqrt{\frac{3}{4/3}} = \frac{3}{2}$.

For our simple model of the proton these small errors are not very important and this representation is adequate.

We generate the start configuration of the 5 partons as if we originally had only 3 quarks that were colour neutral, e.g. one quark of each colour. These emits 2 gluons randomly chosen (though not gluons that are colour neutral), according to $q \to qg$.

A possible start configuration could then be that the red quark emits a gluon with $r\overline{b}$ and the blue emits a gluon with $b\overline{g}$. And we have 1 blue quark, 2 green quarks, 1 gluon with $r\overline{b}$ and another with $b\overline{g}$. If you add these together they will exactly cancel each other and we have a colour neutral configuration.

As we evolve our parton shower we follow the rules of QCD in each vertex. Whenever there is freedom to choose colour is this done randomly. As long as we follow these rules we are guaranteed to have a colour neutral state. However, if we keep all partons, and evolve all this we will get several hundreds of partons in our model and this is not desired. To avoid this we have introduced a x_{min}, as mentioned before. Branchings which produces partons with $x < x_{min}$ are not allowed, but we keep all the partons in the parton shower to keep the colour charge to be zero.

3.6 Number of partons

Here we present a graph showing how the number of partons increase with the virtuality, Q, for two different energy scales. We adjust the energy by changing the variable x_{min} and the lower x_{min} the higher the energy.

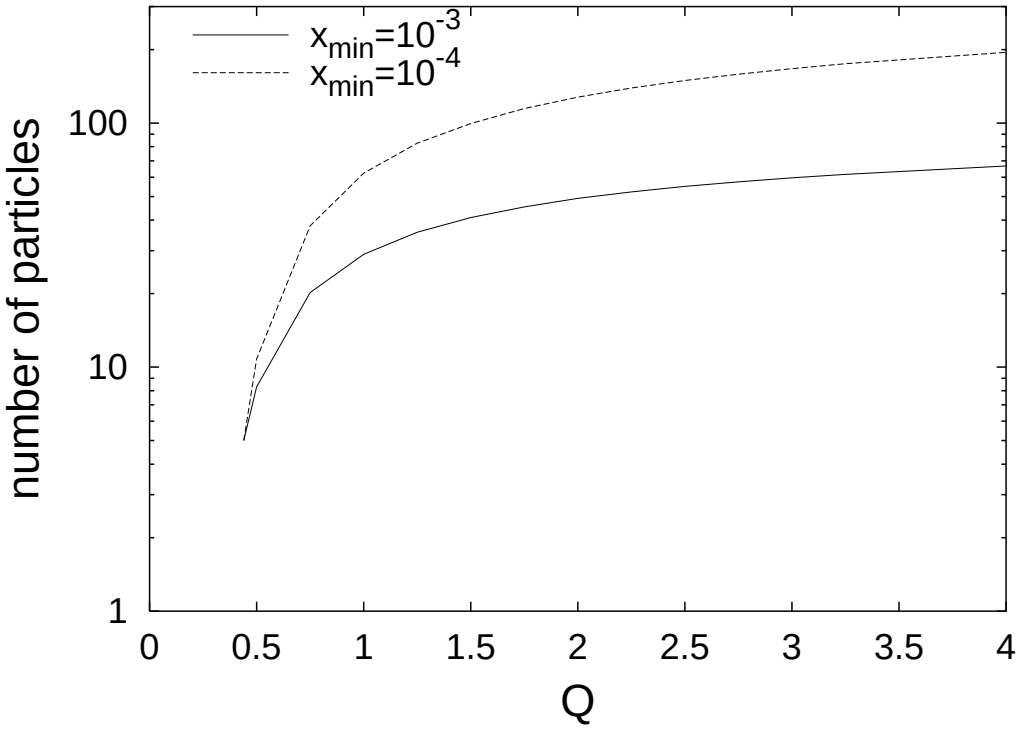

Figure 13: How the number of partons increases with the virtuality, Q.

3.7 A summary of the proton model

Our Model of the proton is made in an exclusive picture. We start at a low Q with only a few partons and let these partons evolve in an iterative process to some Q_{max}. To reduce the number of produced partons we had to introduce a cutoff in the momentum space. The branchings that produces partons with a momentum under this cutoff were not allowed. Despite this rather abrupt cut in the evolution of the parton shower we got a good distribution of partons and their momenta. We have compared our results with GRV in Fig. 8 to Fig. 10 and the total parton shower coincides almost exactly.

We will now use this model to study some different phenomena, but mainly the screening effect.

4 A study of the Model

The primary goal of this section is to study how our model of the proton interacts with a gluon, but also how the radius of the proton varies with the energy of the system, section 4.5. When we are sending a gluon against our proton will we see that the screening effect comes into play and decreases the interaction. We are going to try some different start configurations and see how large the screening effect is, and draw some conclusions of this, section 4.4.

4.1 Introducing the Interference equation

As we discussed in sec 2.3 is the interesting equation when we are studying the interaction of an incoming gluon against the proton the following:

$$A = \frac{|\sum_{k=1}^{n} q_k e^{ipx_k}|^2}{\sum_{k=1}^{n} |q_k|^2}. \tag{29}$$

Since we in our model have assigned both position and colour charge to all partons we can readily use this formula and study how A varies when the incoming gluon has different transverse momentum. According to the theoretical predictions we should have a curve that at low momentum for the gluon is zero and then gradually increase to the maximum value 1 at very high momentum. This is exactly what we have, see Fig. 14.

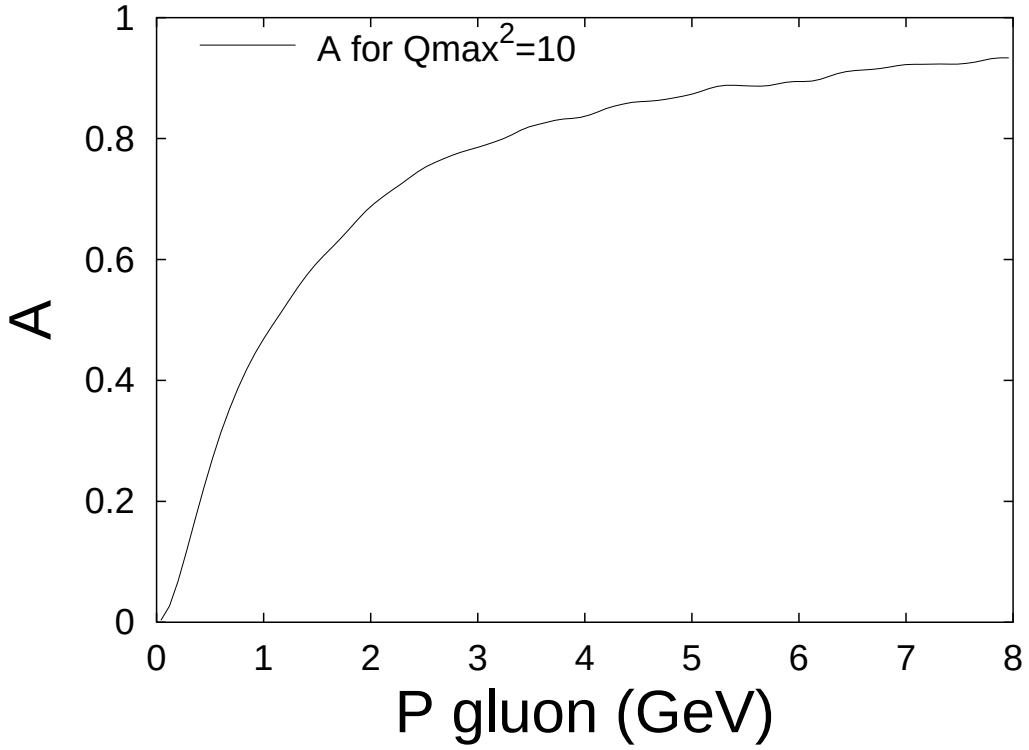

Figure 14: The resolution of the proton increases with the gluon momentum and therefore we approach an incoherent state. $x_{min} = 10^{-3}$

4.2 A running Q

In chapter 4.1 we did the following: We first evolved the parton cascade according to the evolution equations. Then we sent gluons with increasing momenta at the now evolved proton.

Another, more physical, approach would be to probe the proton with a gluon that had approximately the same value on p as the partons has Q. As we mentioned earlier (chapter 2) , is $Q \sim p_\perp$. So this procedure is built upon the principle that a probe can resolve best at its own wavelength (or momentum). In practice this is done by continuously, as we evolve our parton cascade to higher Q, sending in a gluon that has the same p as we have Q at this point.

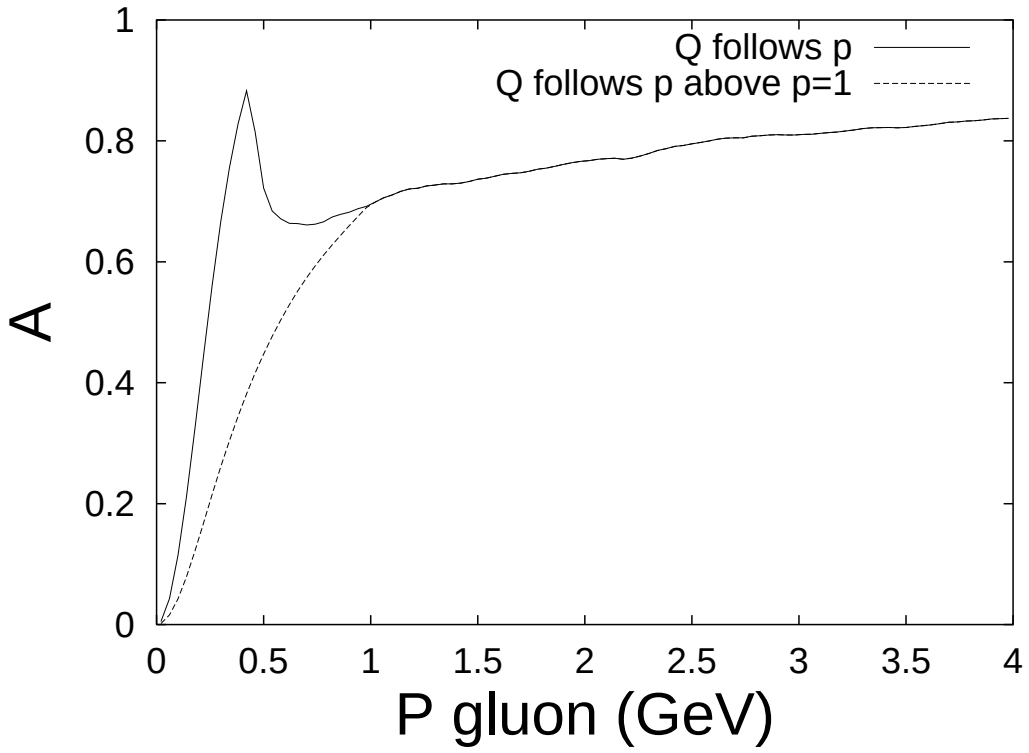

Figure 15: The Interference function $A(p)$ when Q follows the p scale. In the dashed curve is parton shower frozen at $Q = 1$ and downward to avoid the peak at $p = 0.44$. $x_{min} = 10^{-3}$

The peak at $p = 0.44$ in Fig. 15 on the upper curve should not be there. It arises from the fact that when we start our evolution at $Q = 0.44$ we have only 5 partons and these 5 partons have no tendency at all to cluster, unlike the partons produced later in the evolution. Since the physics in this low region is little understood our start configurations can not be checked correctly and it is not certain that the ansatz with only few partons is applicable. What we have done is to take our distribution at a higher Q, in our case at $Q = 1$, and use this distribution all the way down to $Q = 0$. This is similar to what is often done to calculate jet cross-sections with parton distributions not defined below some Q^2. If we do this we get the dashed curve in Fig. 15 and the peak has disappeared.

4.3 Introducing a variable x_{min}

We introduced a cut in the momentum, x_{min}, and partons under this limit was frozen. We did not discuss how this cut was chosen, nor its physical meaning.

If we look at two incoming partons with a momentum of x_1 resp. x_2 we have:

$$\hat{s} = x_1 x_2 s, \tag{30}$$

where s is E_{CM}^2 and $\hat{s}$ is the energy of the subprocess squared. $p_\perp$ can at the most be half of the energy of the subprocess (since we have two partons) and this will mean that we get:

$$p_\perp^2 \leq \frac{\hat{s}}{4} = x_1 x_2 \frac{s}{4} \implies p_\perp^2 \sim x_{min}^2 \frac{s}{4}, \tag{31}$$

that is, we have

$$x_{min}^2 \geq \frac{4p_\perp^2}{s}. \tag{32}$$

This is a somewhat crude calculation, but we see two things here. First, and not so surprising, that the higher total energy we have the better we can resolve partons with small momentum, i.e we get a lower x_{min}. The other thing is that, for a fixed E_{CM}, x_{min} scales linearly with $p_\perp$. So, as we increase the virtuality scale, Q, we should continuously increase x_{min}.

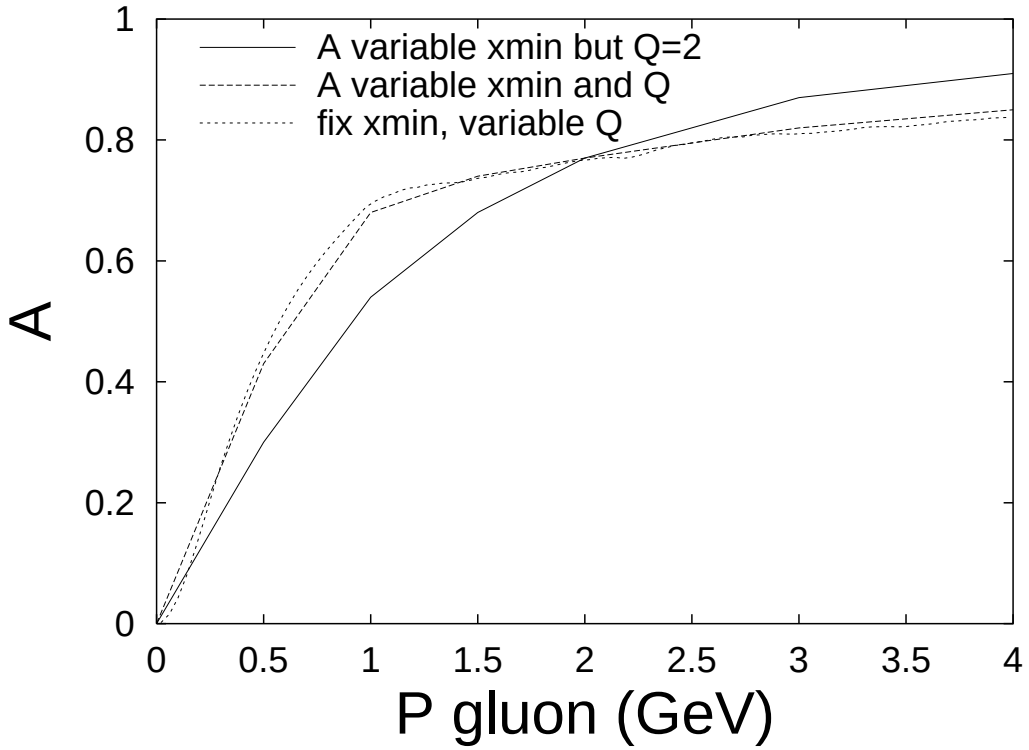

Figure 16: Introducing a variable x_{min}. In the dashed curve is Q running with p while in the other curve is $Q = 2$. We have also included the curve for a fix $x_{min} = 10^{-3}$.

In Fig. 16 we have that $x_{min} = 10^{-3}\, p_\perp$. This factor 10^{-3} can be varied and the curves will be suppressed for smaller factors. In the dashed curve with a running Q have we, as said in chapter 4.2, frozen the parton distribution at $Q = 1$ and downward. As can be seen in Fig. 16 this effect is small.

4.4 The Screening Effect

All the graphs in chapter 4 are a measure of the screening effect since they all tell you how well the gluon can resolve the partons inside the proton. By parameterizing these curves by some function $S(p_\perp)$ you would see the strength of the screening effect and how it increases with the energy. As a reasonable guess, we put:

$$S(p_\perp) = \frac{p_\perp^2}{p_\perp^2 + p_{\perp 0}^2}, \tag{33}$$

where $p_{\perp 0}$ is a free parameter. As long as $p_\perp$ is large is S equal to 1, it is only when $p_\perp$ approaches zero that our correction term comes into play.

In the expression for the cross-section σ_{jet} we had

$$\mathrm{d}\sigma_{jet} = \int \mathrm{d}x_1 f(x_1, p_\perp^2) \int \mathrm{d}x_2 f(x_2, p_\perp^2) \int \frac{\mathrm{d}\hat{\sigma}}{\mathrm{d}p_\perp^2} \mathrm{d}p_\perp^2, \tag{34}$$

or, if we rewrite it a little

$$\frac{\mathrm{d}\sigma_{jet}}{\mathrm{d}p_\perp^2} = \frac{\mathrm{d}\hat{\sigma}}{\mathrm{d}p_\perp^2} \int \mathrm{d}x_1 f(x_1, p_\perp^2) \int \mathrm{d}x_2 f(x_2, p_\perp^2). \tag{35}$$

It is the first term in this expression that has a singularity as $p_\perp \to 0$ since it goes like $1/p_\perp^4$. By introducing $S(p_\perp)$ (squared since we have two partons) into Eq (35) this singularity disappears and we get a finite value:

$$\begin{aligned} \frac{\mathrm{d}\sigma_{jet}}{\mathrm{d}p_\perp^2} &= S(p_\perp)^2 \frac{\mathrm{d}\hat{\sigma}}{\mathrm{d}p_\perp^2} \int \mathrm{d}x_1 f(x_1, p_\perp^2) \int \mathrm{d}x_2 f(x_2, p_\perp^2) \\ &= \frac{p_\perp^4}{(p_\perp^2 + p_{\perp 0}^2)^2} \frac{\mathrm{d}\hat{\sigma}}{\mathrm{d}p_\perp^2} \int \mathrm{d}x_1 f(x_1, p_\perp^2) \int \mathrm{d}x_2 f(x_2, p_\perp^2) \\ &\sim \frac{1}{(p_\perp^2 + p_{\perp 0}^2)^2} \int \mathrm{d}x_1 f(x_1, p_\perp^2) \int \mathrm{d}x_2 f(x_2, p_\perp^2) \end{aligned} \tag{36}$$

When introducing the screening function $S(p_\perp)$ we adjust the parameter $p_{\perp 0}$ e.g., so that $S(p_\perp)$ coincides with our curve at $A = 0.5$, see Fig. 17. By doing this for different energies we can plot how the screening effect varies by the energy. We change the energy of the parton shower by changing x_{min} since we had the relation that $x_{min} \sim 1/E_{CM}$.

The curve that has a fix Q can better be fitted with our screening function than the one with a running Q, see Fig. 17. This indicates a shortcoming either of the model or in the ansatz of S. We will use a fix Q mostly, to allow a more sensible comparison.

By plotting $p_{\perp 0}$ versus $1/x_{min}$ we get a good measure of how the screening effect varies by the energy. We have, in Fig 18 done this for some different start configurations and also some different evolution conditions. Since we do not know how much the partons separate themselves in a branching we will also look at events where the splitting is twice the size of Eq (24)

1. A fix $Q = 2$ and a branching according to Eq (24)
2. A fix $Q = 2$ and a branching twice the size of Eq (24)
3. A running Q and a branching twice the size of Eq (24)

We see in Fig. 18 that $p_{\perp 0}$ increases as the energy of the system is increased. By this we get that σ_{jet} increase slower than for a fixed $p_{\perp 0}$ and we get a nicer behavior than in Fig 4.

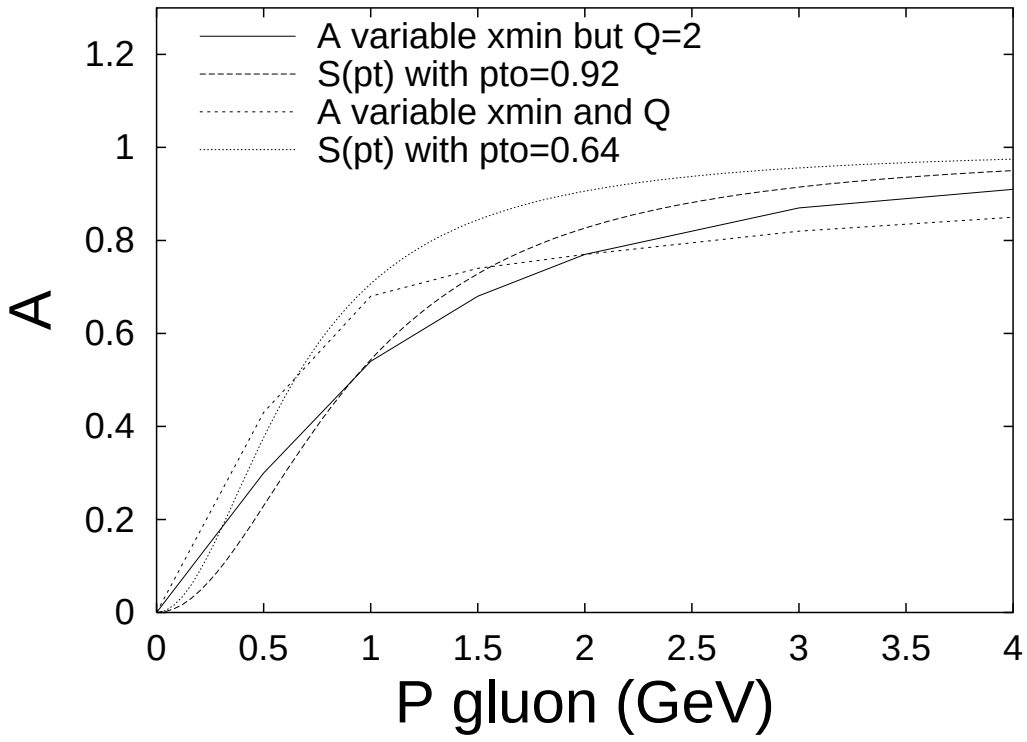

Figure 17: The screening function S($p_\perp$) fitted to A. Our parameterization of the screening function can best be fitted to the curve with a fix Q.

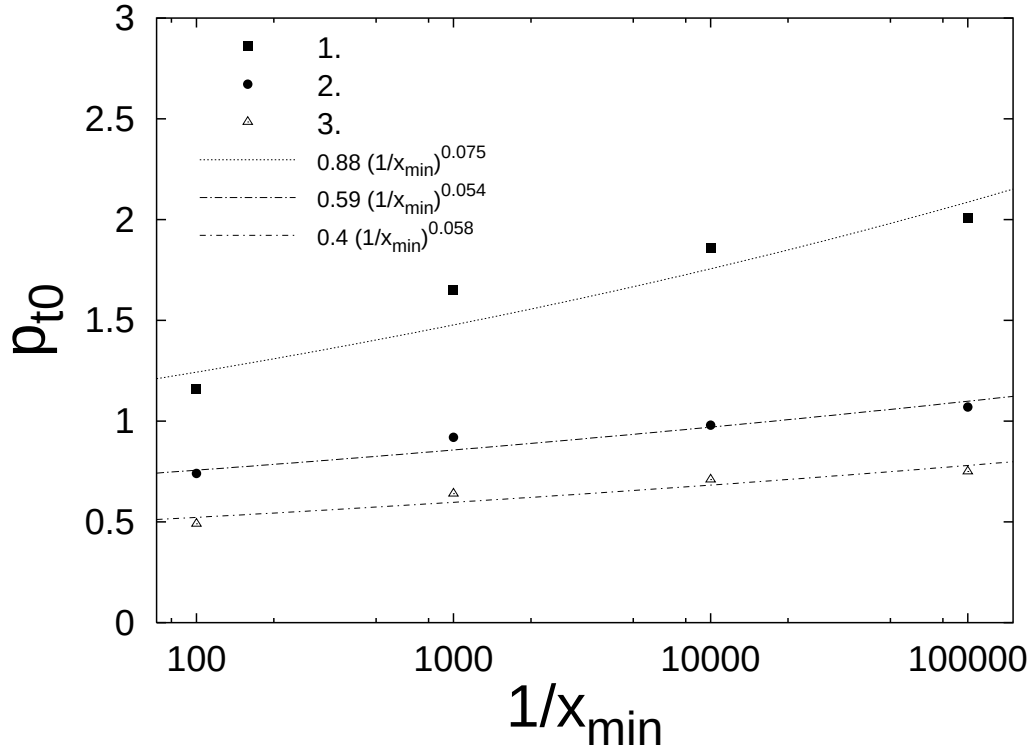

Figure 18: How $p_{\perp 0}$ varies with the energy for different start configurations. Scenarios 1,2 and 3 according to the notation in the text.

4.5 The Radius of the Proton in our Model

As another application of our model we are going to look at how the radius of our model of the proton evolves as we increase the energy of the system.

We do this by plotting the parton density function $f(r)$:

$$f(r) = \frac{1}{r}\frac{\mathrm{d}n_{partons}}{\mathrm{d}r} = \frac{\mathrm{d}n_{partons}}{\mathrm{d}^2 r}, \tag{37}$$

the phase-space factor $1/r$ is introduced to avoid having a vanishing distribution at $r = 0$. The center, from which the distance r is calculated, is simply the total average of the position of all partons.

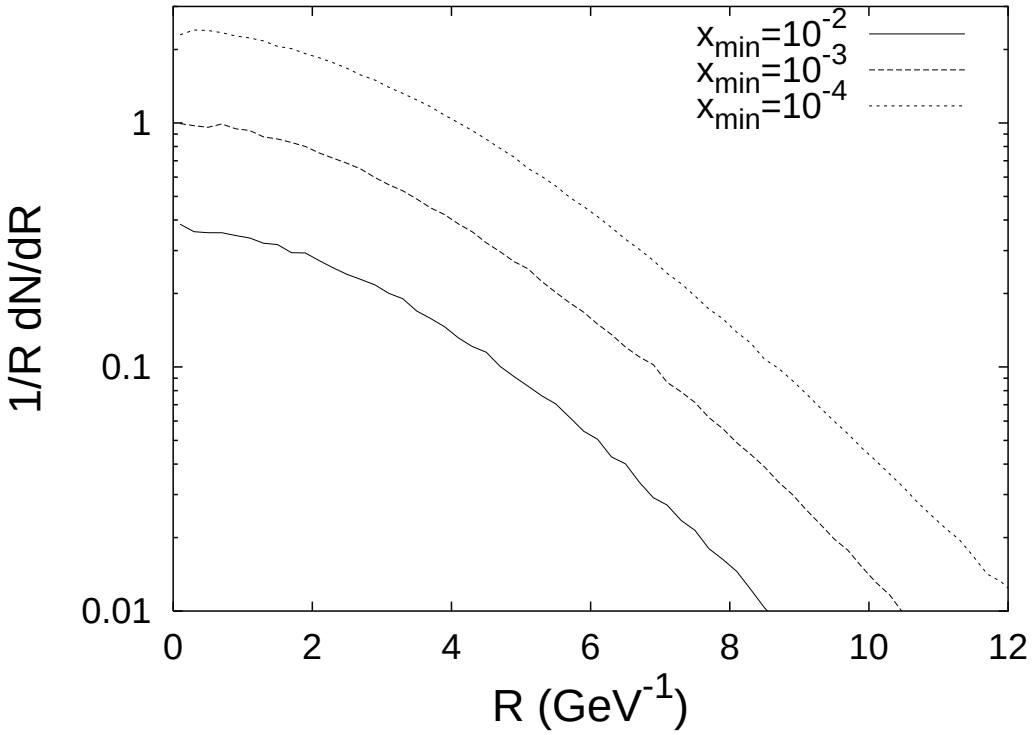

Figure 19: How the radius of our proton model varies with the energy.

By defining some lowest density of the proton it is easy to define a radius as the distance from origo to the point on the curve at this lowest density. To vary the energy we once again changes the parameter x_{min}, see Fig 19. Here the density function is plotted for some different x_{min}. As is expected, the radius increases with the energy. We see that the curves in Fig 19 are almost parallel to each other. This means that the partons stays rather close to their original parton mother. Though a closer examination of Fig 19 shows that the curves spreads towards larger R. This is an indication of some diffusion, i.e. partons that have traveled far from their original position.

5 Summary and Conclusions

This paper is divided in two main parts:

1. The Proton Model
2. The Studies of the Model

In the first part we describe how the model is constructed and which conditions we have made upon it.

The model is iterative in its structure; we start with a configuration of only 5 partons. These are then evolved towards higher virtuality scales Q to some Q_{max} where we stop the evolution. The evolution is done in an exclusive picture i.e. we follow each parton by simulating the probability for a branching by random numbers. To know the probability for a branching we use the Altarelli-Parisi splitting kernels.

If we allowed all partons there would be infinitely many in our model, and this is not possible. To avoid this we introduced a cutoff in momentum space. The branchings that produces partons with a momentum below this x_{min} were not allowed, all the partons are still kept into the parton shower though. Despite this rather abrupt cutoff, the distribution of the partons is not changed significantly.

We have also made the model so that it is always colour neutral. This is done by having a colour neutral start configuration. Then, as we evolve, the rules of QCD are followed and no partons are thrown away.

All partons were assigned a transverse position in the coordinate space and a longitudinal value of the momentum. This is done to try to avoid difficulties from the Heisenberg uncertainty principle.

We have compared our model to the model by the GRV group, see Fig. 8 to Fig. 10. Our model cannot compete with GRV but we have a rather good agreement between the two models, especially at high Q.

In the second part of this paper we studied the so called screening effect with our model. The screening effect is that the partons will screen each other so the charge seen from outside the proton will be lower than the naive incoherent sum. By using our model as a target we sent gluons with different momentum at the proton.

We made some different assumptions of how the gluon interact with the proton model:

- A running Q: That the incoming gluon will react mostly with partons with Q (and thereby $p_\perp$) equal to the gluon momentum
- A running x_{min}: The cutoff variable x_{min} should vary with the Q scale.
- The distance between the partons: When a branching occurs the distance between the daughters are decided by Eq (24), this is varied

The different curves of this is presented in Fig. 18. We see that there are some differences, but the qualitative behavior is the same. We clearly have the screening effect and the σ_{jet} will be better behaved than in Fig. 4.

Acknowledgement

I would first of all like to thank my supervisor Torbjörn Sjöstrand for his support and patience as well as for introducing me to this subject. I would also like to thank the rest of the department who have helped me during this time. And of course my family and friends for their support and encouragement.

References

[1] H-U. Bengtsson, G. Gustafson and L. Gustafson, "Kvarken och universum", Corona (Malmö, 1994).

[2] Gordon Kane, "Modern Elementary Particle Physics", Addison-Wesley (Massachusetts, 1993)

[3] G. Altarelli and G. Parisi, Nucl. Phys. Rev. **B126** (1977) 298; Yu.L. Dokshitzer, Sov. Phys. JETP **46** (1977) 641

[4] A.D. Martin, R.G. Roberts, W.J. Stirling and R.S. Thorne, Eur.Phys.J **C4:463-496** (1998)

[5] CTEQ Collaboration, H.L. Lai et al.,hep-ph/9903282

[6] T. Sjöstrand and M. van Zijl, Phys. Rev. **D36** (1987) 2019

[7] CDF Collaboration, F. Abe et al., phys. Rev. Lett. **79** (1997) 584.

[8] UA2 Collaboration, J. Aletti et al., Phys. Lett. **B268** (1991) 145.

[9] A. Donnachie and P.V. Landshoff, Phys. Lett. **B209** (1988)90.

[10] T. Sjöstrand, Computer Phys. Common. **82** (1994) 74.

[11] M. Glück, E. Reya and A. Vogt: Z. Phys **C 67, 433-447** (1995)

[12] G. Parisi and R. Petronzio: Phys. Lett **62B** (1976) 331; V.A Novikov, M.A. Shifman, A.I. Vainshtein and V.I. Zakharov: JETP Lett. **24** (1976) 341; Ann. Phys. (N.Y.) 105 (1977) 276; M. Glück and E. Reya: Nucl.Pys. **B130** (1977) 76

[13] M. Glück, E. Reya and A. Vogt,"Radiatively Generated Distributions for High Energy Collisions" , Institut for Physics: (Dortmund, 1989)